

# Electromagnetic actuation and microchannel engineering of a polymer micropen array integrated with microchannels and sample reservoirs for biological assay patterning

Maesoon Im<sup>a)</sup>

*Division of Electrical Engineering, School of Electrical Engineering and Computer Science, Korea Advanced Institute of Science and Technology (KAIST), Daejeon 305-701, Republic of Korea*

Il-Joo Cho

*Department of Electrical and Computer Engineering, University of Minnesota, Minneapolis, Minnesota 55455, USA*

Kwang-Seok Yun

*Department of Electronic Engineering, Sogang University, Seoul 121-742, Republic of Korea*

Euisik Yoon

*Department of Electrical and Computer Engineering, University of Minnesota, Minneapolis, Minnesota 55455, USA*

(Received 25 July 2007; accepted 2 September 2007; published online 20 September 2007)

A polymer (SU-8) micropen array was fabricated for application to biological assay patterning. The micropen, which is integrated with a microchannel and a sample reservoir, can be actuated by Lorentz force induced on an integrated metal actuator. Current to a metal line deflects the micropen up to 1.8  $\mu\text{m}$  by electromagnetic force induced from external permanent magnets. Red ink is loaded in the reservoir and is automatically drawn to the end point of the microchannel by capillary force. A red-ink dot with a diameter of 11  $\mu\text{m}$  was successfully placed onto paper by the fabricated micropen. © 2007 American Institute of Physics. [DOI: 10.1063/1.2787971]

As the volume of a biological assay decreases and its throughput increases, the cost of the assay can be significantly reduced.<sup>1</sup> Accordingly, numerous studies have been performed in an effort to develop more efficient biological assay patterning techniques, such as those that utilize ink-jet printing,<sup>2</sup> and cantilever-based technologies<sup>3–8</sup> as with dip pen nanolithography.<sup>1</sup>

For continuous biological assay patterning in a large area, a constant supply of liquid samples is necessary. Fountain pen nanolithography, in which a microchannel is embedded in a cantilever and a few cantilevers share a reservoir, was proposed by Kim *et al.* for the first time.<sup>3</sup> Functional devices with similar methods of operation have also been reported.<sup>4,5</sup>

Due to a lack of integrated actuators on the cantilever, these approaches can experience a slow patterning speed. Many studies focusing on the integration of actuators on the cantilever using either thermal actuation<sup>6,7</sup> or electrostatic actuation<sup>8</sup> have been reported. However, a working device that is integrated with a microchannel and has a reservoir as well as an actuator has not been reported subsequent to the earlier proposal by Kim *et al.*

In this study, a polymeric microcantilever structure integrated with a microchannel, a reservoir, and an electromagnetic actuator is described.<sup>9</sup> Samples are supplied spontaneously and continuously from the reservoir to the end of the micropen by capillary transport. This micropen can pattern various biological samples in a designated spot with individual actuation by Lorentz force in an array form.

Initially, the micropen is not in contact with the substrate. In order to deliver a biological sample to a designated spot in the substrate, the micropen is actuated and makes contact with the substrate. After delivering the biological sample, the current is disconnected and the micropen is pulled back from the substrate and returned to its initial position. If any nonuniform distribution exists in the initial gaps between the substrate and the micropens in an array, an adequate amount of current in the appropriate direction can be applied to maintain the desired identical distances. Among various actuation mechanisms, electromagnetic actuation is most suitable for such adjustments due to its linearity.

SU-8 was chosen as the structural material for the following three reasons: First, SU-8 is known to be compatible with most bioassays. Hence, it is a suitable candidate for microchannel structures in biological assay patterning. Second, due to the photodefinable feature of SU-8, the micropen area can be formed simply using a photolithographic process without additional etching steps. Finally, SU-8 has low Young's modulus. Young's modulus of SU-8 (approximately 4.4 GPa) (Ref. 10) is considerably lower than that of Si (170–190 GPa) (Refs. 10 and 11) or Si<sub>3</sub>N<sub>4</sub> (224.6–295 GPa),<sup>6,12</sup> which is used as a structural material in most existing microcantilever structures.<sup>3,5–7,11</sup>

Figure 1 shows scanning electron microscope images of the micropen array (500  $\mu\text{m}$  long, 120  $\mu\text{m}$  wide, and 6  $\mu\text{m}$  thick) with 240  $\mu\text{m}$  spacing. The fabrication process of the micropen array is available in the literature.<sup>9</sup> The micropen is fabricated on a sacrificial layer of Cr/Au/Cr (5 nm/50 nm/20 nm) that is sputtered on a silicon wafer. A Ti/Au (20 nm/1  $\mu\text{m}$ ) metal line for electromagnetic actuation exists between two SU-8 layers (2  $\mu\text{m}$  thick bottom layer, 4  $\mu\text{m}$  thick top layer) in a sandwich structure. The

<sup>a)</sup> Author to whom correspondence should be addressed; electronic mail: maesoon.im@gmail.com

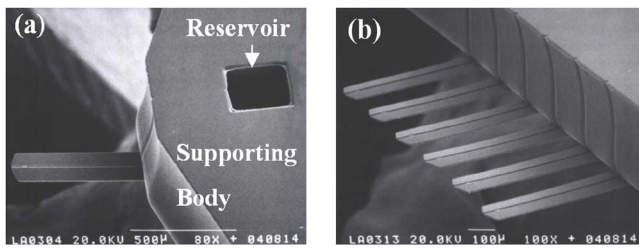


FIG. 1. Scanning electron microscope photographs of the fabricated micro-pen array. The length, width, and thickness of the micropen are 500, 120, and 6  $\mu\text{m}$ , respectively. (a) The supporting body (500  $\mu\text{m}$  thick) and the reservoir with an area of  $300 \times 300 \mu\text{m}^2$ . The capacity of this reservoir is roughly 45 nL. (b) An array of six micropens with a spacing of 240  $\mu\text{m}$ . As each micropen has a reservoir and an integrated actuator, the micropens can be controlled individually to pattern six different biological samples.

supporting body of a 500  $\mu\text{m}$  thick SU-8 layer includes deep reservoirs to store biological samples. In the final releasing step, the high electronegativity difference between chromium and gold allows the chromium to be rapidly etched away in an electrochemical reaction.<sup>13</sup> While similar processes have been reported<sup>14,15</sup> for sensor applications, this approach is applied in an actuator including microfluidic channel engineering.

A schematic diagram of the proposed micropen with its actuation mechanism is shown in Fig. 2(a). The micropen is controlled with a simple electromagnetic actuator that consists of a gold metal line and permanent magnets.<sup>16,17</sup> High actuation voltage is required in the case of electrostatic actuation,<sup>8,18</sup> and the deflected cantilever position is unstable after the actuation voltage exceeds a threshold.<sup>19</sup> In contrast, electromagnetic actuation can generate a large force with a lower operating voltage with greater power consumption while being immune to cross-talk caused by fringing electric fields. Additionally, plastic deformation may occur when thermal actuation is used, potentially resulting in damage to

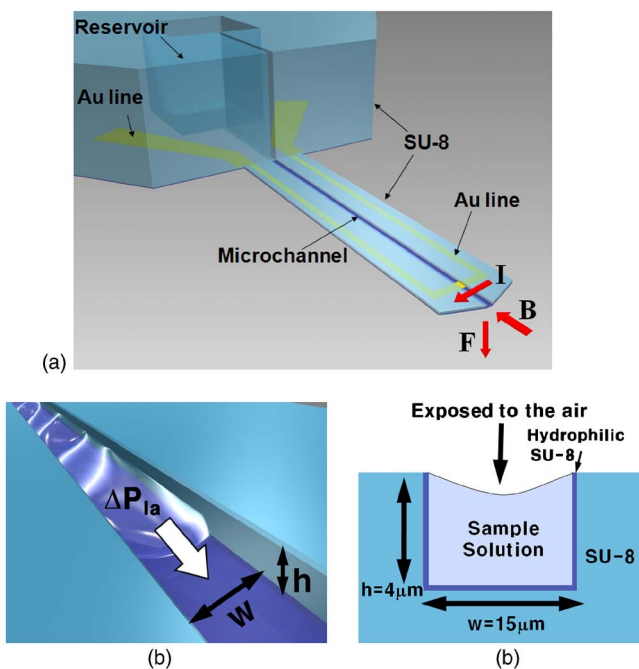
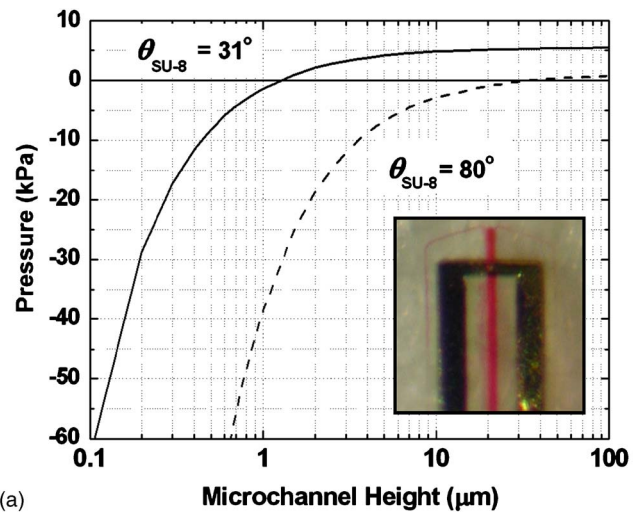
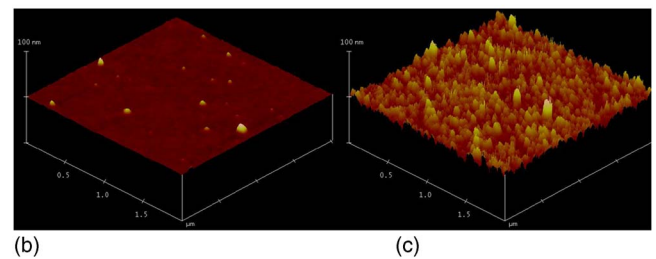


FIG. 2. (Color online) (a) Schematic view of the proposed micropen and its actuation mechanism. (b) Overview of the microchannel schematic. (c) Cross-sectional view of the microchannel. Three walls are SU-8, whereas one side is exposed to air.



(a)



(b)

(c)

FIG. 3. (Color online) (a) Capillary force as a function of the microchannel height for a microchannel width of 15  $\mu\text{m}$  is increased by plasma treatment. (Inset) Red ink was drawn up to the end point of the microchannel from the reservoir by capillary force. (b) Atomic force microscope images of SU-8 surfaces before an oxygen plasma treatment and (c) after an oxygen plasma treatment. The mean roughness is shown to have increased from 0.318 to 2.627 nm.

micropens made of SU-8, although thermal actuation provides a considerable amount of deflection with less power consumption.<sup>7</sup> Plastic deformation of SU-8 cantilevers is observed above 180  $^{\circ}\text{C}$ .<sup>11</sup> Therefore, electromagnetic actuation was selected for SU-8 micropens to allow for the use of low voltage and to avoid irreversible plastic deformation of SU-8.

The proposed micropen houses a microchannel with three SU-8 walls and the remaining side is exposed to air, as shown in Figs. 2(b) and 2(c). The pressure drop across the horizontal liquid-air interface can be expressed in terms of the channel dimensions and contact angles, as follows:<sup>20</sup>

$$\Delta P_{\text{la}} \approx \left( \frac{2}{w} + \frac{1}{h} \right) \gamma \cos \theta_{\text{SU-8}} + \frac{1}{h} \gamma \cos \theta_{\text{air}}. \quad (1)$$

Here,  $\gamma$  is the surface energy per unit area,  $\theta_{\text{air}}$  and  $\theta_{\text{SU-8}}$  are the contact angles of air and SU-8, and  $w$  and  $h$  are the width and height of the microchannel, respectively. In order to obtain an absorptive capillary force for water, the microchannel should have a positive pressure force for water, the above equation. As the water contact angle of air is 180 $^{\circ}$ ,  $\cos \theta_{\text{air}}$  has a minimum value of  $-1$ .<sup>21</sup> The contact angle of SU-8 was measured as 80 $^{\circ}$ , and the surface energy per unit area of red ink was measured as 0.048 N/m using a contact angle analyzer (Phoenix 300, Surface Electro Optics Co. Ltd, Suwon, Korea). Under consideration of a 15  $\mu\text{m}$  wide microchannel, the pressure drop in the microchannel was calculated for various microchannel heights and is plotted in Fig. 3(a) (dashed line). For the automatic transport of biological

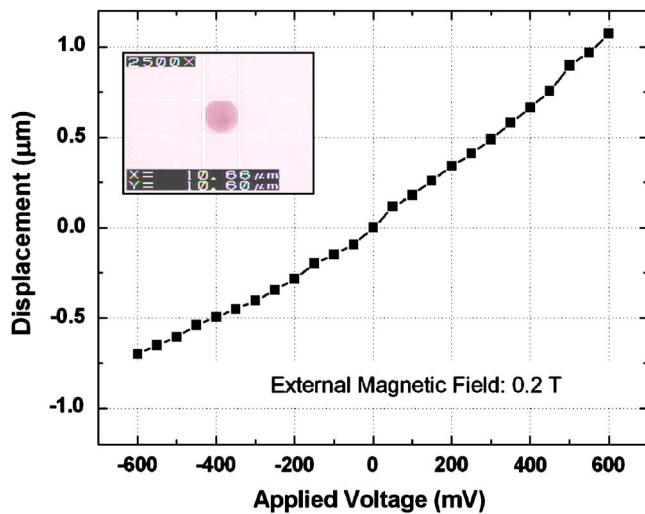


FIG. 4. (Color online) Measured deflection of the micropen as a function of applied current: (Inset) Microscope image of a red-ink dot (approximately  $11 \mu\text{m}$  in diameter) placed by the fabricated micropen.

samples through the microchannel, the pressure drop should be adjusted so that it is positive. Through an oxygen plasma treatment, the SU-8 surface is highly activated due to the additional oxygen and the decreased amount of carbon.<sup>22</sup> This lends more hydrophilic characteristics. Additionally, the plasma-treated SU-8 surface is much coarser than the original surface, as shown in Figs. 3(b) and 3(c). This rough surface amplifies the hydrophilic behavior.<sup>23</sup> The contact angle of SU-8 is decreased to  $31^\circ$  after the plasma treatment, and the adjusted pressure drop is plotted in Fig. 3(a) (solid line). The pressure drop increases from  $-8.79$  to  $3.77$  kPa for a microchannel height of  $4 \mu\text{m}$ , and the resultant capillary force carries samples automatically from the reservoir to the end point of the micropen. Red ink was used in a visual inspection of the capillary force with respect to its ability to draw the samples. As clearly shown in the inset of Fig. 3(a), red ink was drawn up to the end point of the microchannel from the reservoir by capillary force. It does not overflow the microchannel, as the plasma treatment of the SU-8 occurred only in the microchannel. Outside of the microchannel, SU-8 continues to maintain a large contact angle.

For electromagnetic actuation of the fabricated micropen, two permanent magnets were used to apply a magnetic field of  $0.2$  T. When the current flows in the gold metal line, the micropen is deflected upward or downward depending on the current direction. The deflection of the micropen was measured using a laser doppler vibrometer (Polytec GmbH, Waldronn, Germany). The measured displacement is plotted as a function of the applied current in Fig. 4. With an applied voltage of  $\pm 600$  mV, the deflection of the fabricated micropen was measured as  $-0.7$  or  $1.1 \mu\text{m}$  in each direction. This deflection range can be further improved. First, the external magnetic fields can be increased with stronger permanent magnets. Second, additional metal lines can be integrated on the micropen. It should be noted that the increase in the magnitude of the current is limited, as a high level of current will induce Joule heating. This in turn may have a thermal effect such as plastic deformation of the device, electrolysis of the sample solution, or even degradation of the biological

samples. The average resistance of the fabricated micropens is  $5.0 \Omega$ , and the power consumption can be estimated as  $72$  mW for an applied voltage of  $\pm 600$  mV. Instead of electrolysis, which takes place above  $1.2$  V,<sup>24</sup> the boiling of water is observed when a higher level of current is applied to the metal line.

The spring constant was estimated as  $1.9$  N/m, and the resonance frequency was measured as  $7.3$  kHz. By individual control of the micropens in the array, much faster patterning speeds can be achieved and various biological samples can be simultaneously patterned, as they can be separately stored in the dedicated reservoirs of each micropen.

A red-ink dot approximately  $11 \mu\text{m}$  in diameter was placed onto a sheet of paper by actuating the fabricated micropen, as shown in the inset of Fig. 4. This demonstrates that subpicoliter patterning of biological assay is possible. The size of the deposited red-ink dot can be further minimized by reducing the microchannel size. In addition, a biological assay can be patterned in various shapes with a computer-controlled XYZ motion handling system.

<sup>1</sup>D. S. Ginger, H. Zhang, and C. A. Mirkin, *Angew. Chem., Int. Ed.* **43**, 30 (2004).

<sup>2</sup>T. Laurell, L. Wallman, and J. Nilsson, *J. Micromech. Microeng.* **9**, 369 (1999).

<sup>3</sup>K.-H. Kim, C. Ke, N. Moldovan, and H. D. Espinosa, *Proceedings of the Fourth International Symposium on MEMS and Nanotechnology, 2003*, p. 235.

<sup>4</sup>P. Belaubre, M. Guirardel, V. Leberre, J.-B. Pourciel, and C. Bergaud, *Sens. Actuators, A* **110**, 130 (2004).

<sup>5</sup>S. Deladi, J. W. Berenschot, N. R. Tas, G. J. M. Krijnen, J. H. de Boer, M. J. de Boer, and M. C. Elwenspoek, *J. Micromech. Microeng.* **15**, 528 (2005).

<sup>6</sup>D. Bullen, X. Wang, J. Zou, S.-W. Chung, C. A. Mirkin, and C. Liu, *J. Microelectromech. Syst.* **13**, 594 (2004).

<sup>7</sup>X. Wang, D. A. Bullen, J. Zou, C. Liu, and C. A. Mirkin, *J. Vac. Sci. Technol. B* **22**, 2563 (2004).

<sup>8</sup>D. Bullen and C. Liu, *Sens. Actuators, A* **125**, 504 (2006).

<sup>9</sup>M. Im, I.-J. Cho, K.-S. Yun, and E. Yoon, *Proceedings of the 13th International Conference on Solid-State Sensors, Actuators and Microsystems, 2005*, p. 1588.

<sup>10</sup>G. Genolet, J. Brugger, M. Despont, U. Drechsler, P. Vettiger, N. F. de Rooij, and D. Anselmetti, *Rev. Sci. Instrum.* **70**, 2398 (1999).

<sup>11</sup>A. Johansson, O. Hansen, J. Hales, and A. Boisen, *J. Micromech. Microeng.* **16**, 2564 (2006).

<sup>12</sup>J. Zou, X. Wang, D. Bullen, K. Ryu, C. Liu, and C. A. Mirkin, *J. Micromech. Microeng.* **14**, 204 (2004).

<sup>13</sup>G. Genolet, Ph.D. thesis, Ecole Polytechnique Fédérale de Lausanne, 2001.

<sup>14</sup>J. Thaysen, A. D. Yalcinkaya, P. Vettiger, and A. Menon, *J. Phys. D* **35**, 2698 (2002).

<sup>15</sup>A. Johansson, M. Calleja, P. A. Rasmussen, and A. Boisen, *Sens. Actuators, A* **123–124**, 111 (2005).

<sup>16</sup>D. W. Lee, T. Ono, and M. Esashi, *Sens. Actuators, A* **83**, 11 (2000).

<sup>17</sup>I.-J. Cho, K.-S. Yun, H.-K. Lee, J.-B. Yoon, and E. Yoon, *Proceedings of the 15th IEEE MEMS, 2002*, p. 54.

<sup>18</sup>R. Legtenberg, J. Gilbert, S. D. Senturia, and M. Elwenspoek, *J. Microelectromech. Syst.* **6**, 257 (1997).

<sup>19</sup>G. T. A. Kovacs, *Micromachined Transducers Sourcebook* (McGraw-Hill, New York, 2000), p. 280.

<sup>20</sup>K.-S. Yun and E. Yoon, *Biomed. Microdevices* **7**, 35 (2005).

<sup>21</sup>A. B. D. Cassie, *Discuss. Faraday Soc.* **3**, 11 (1948).

<sup>22</sup>F. Walther, P. Davydovskaya, S. Zürcher, M. Kaiser, H. Herberg, A. M. Giggler, and R. W. Stark, *J. Micromech. Microeng.* **17**, 524 (2007).

<sup>23</sup>R. N. Wenzel, *Ind. Eng. Chem.* **28**, 988 (1936).

<sup>24</sup>C. Neagu, H. Jansen, H. Gardeniers, and M. Elwenspoek, *Mechatronics* **10**, 571 (2000).